EXTRAPOLATED VECTOR MAGNETIC FIELD DISTRIBUTIONS OF AR 6659 IN JUNE 1991 BY BOUNDARY ELEMENT METHOD OF CONSTANT-α FORCE-FREE FIELD

YIHUA YAN and QING YU
Beijing Astronomical Observatory, Chinese Academy of Sciences, Beijing 100080, China
and
TONGJIANG WANG
Department of Astronomy, Nanjing University, Nanjing 210008, China

(Received 10 May, 1994; in final form 8 March, 1995)

Abstract. Using the boundary element method (BEM) for constant-α, force-free fields, the vector magnetic field distributions in the chromosphere of a flare-productive active region, AR 6659 in June 1991, are obtained by extrapolating from the observed vector magnetograms at the photosphere. The calculated transverse magnetic fields skew highly from the photosphere to the chromosphere in the following positive polarity sunspot whereas they skew only slightly in the main preceding sunspot. This suggests that more abundant energy was stored in the former area causing flares. Those results demonstrate the validity of the BEM solution and the associations between the force-free magnetic field and the structure of the AR 6659 region. It shows that the features of the active region can be revealed by the constant-α force-free magnetic field approximation.

1. Introduction

The flare-productive active region AR 6659 in June 1991 has been studied by Wang (1993), Zirin and Wang (1993), and Zhang and Wang (1994), where the evolution of vector magnetograms and their relationship with flares were demonstrated through the development of magnetic shear and changes of the vector magnetic fields and flares, attempting to analyze the physical nature of the event.

In this paper we would like to study the magnetic field structures above the active region by the proposed boundary element formulation (BEM), which has a unique solution and a finite energy content for constant-α, force-free fields (Yan, Yu, and Kang, 1991), and is discussed in detail in Yan (1995).

The present paper is divided into several parts: (a) in Section 2 we first establish the system used for analyzing the active region and the preparation of Huairou observatory photospheric vector magnetograms with the 180° ambiguity removed; (b) then in Section 3, we briefly describe the proposed model and its BEM solution which is discussed in detail in Yan (1995); (c) in Section 4, we finally demonstrate the chromospheric vector magnetograms extrapolated by solving for force-free fields above AR 6659 using BEM, and discuss the associations between the magnetic fields and Hβ filtergrams.

Solar Physics **159:** 115–126, 1995.

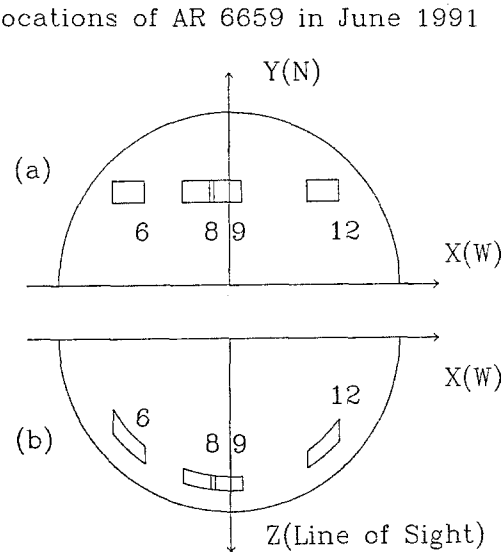

Fig. 1. Description of the locations of AR 6659 on different days in orthogonal coordinates displayed from both (a) front view and (b) top view. Numbers 6, 8, 9, and 12 indicate the dates: 6, 8, 9, and 12 June, respectively. The Y axis is to the north, and X to the west, whereas the Z axis is parallel to the line of sight.

2. Vector Magnetic Fields of AR 6659 in June 1991

A number of photospheric **B** vector magnetograms in June 1991 of the flare-productive active region AR 6659 were observed by the Huairou Solar Observing Station of Beijing Astronomical Observatory. They serve as the boundary condition in the present research. Figure 1 shows the front and top views of locations of the active region in orthogonal coordinates on different days, and 6, 8, 9, and 12 indicate the dates: June 6, 8, 9, and 12, respectively. The Y-direction is the north, and X-direction is the west, whereas the Z-direction is parallel to the line of sight.

Figure 2(a–d) shows the observed photospheric vector magnetic fields taken at 5324 Å on 6, 8, 9, and 12 June, 1991, respectively, corresponding to the photospheric boundary. The longitudinal component is represented by iso-magnetic field contours with thick (thin) lines indicating N (S) polarity of the values ± 40, ± 160, ± 640, ± 1280, ± 1920, ± 2240, ± 2560, and ± 2880 G, whereas the transverse components are represented by arrow bars with each length indicating the transverse field value at a scale of 250 G per unit length.

It can be seen that the main preceding sunspot of the active region was of negative longitudinal polarity, whereas near its boundary to the opposite polarity, or places near neutral lines, highly sheared transverse magnetic fields were observed. Due to newly emerged sunspots moving through older magnetic field configurations, a number of flares occurred (Zirin and Wang, 1993).

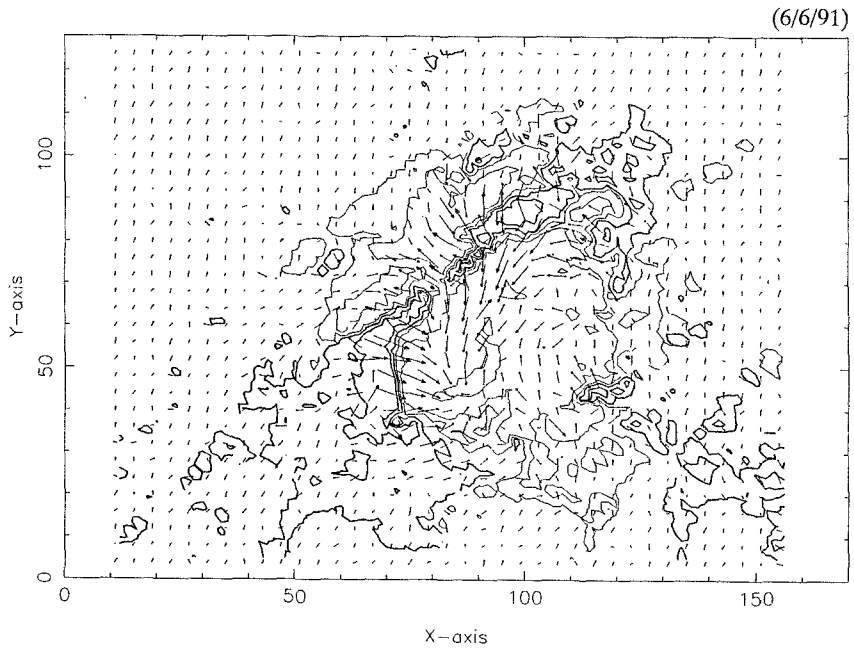

Fig. 2a.

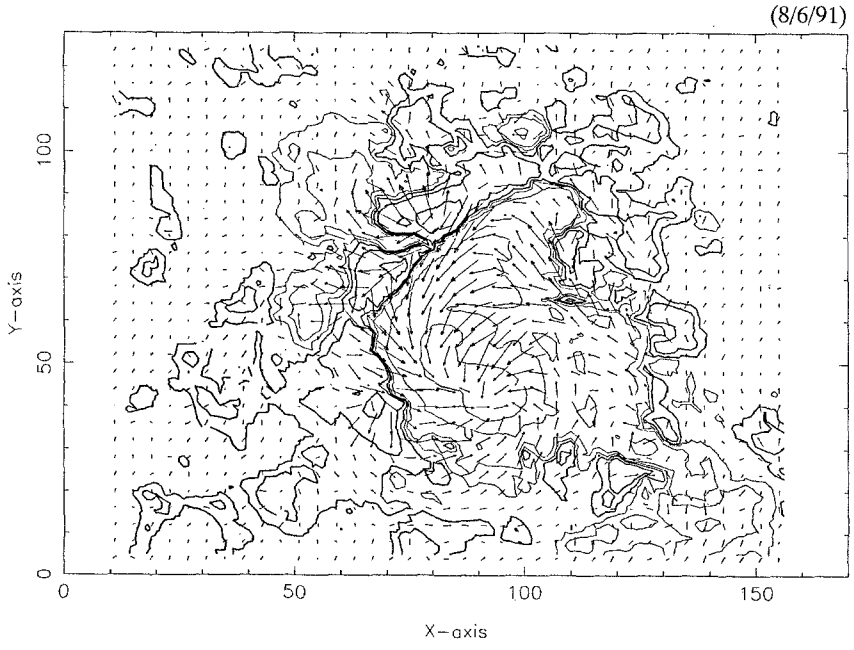

Fig. 2b.

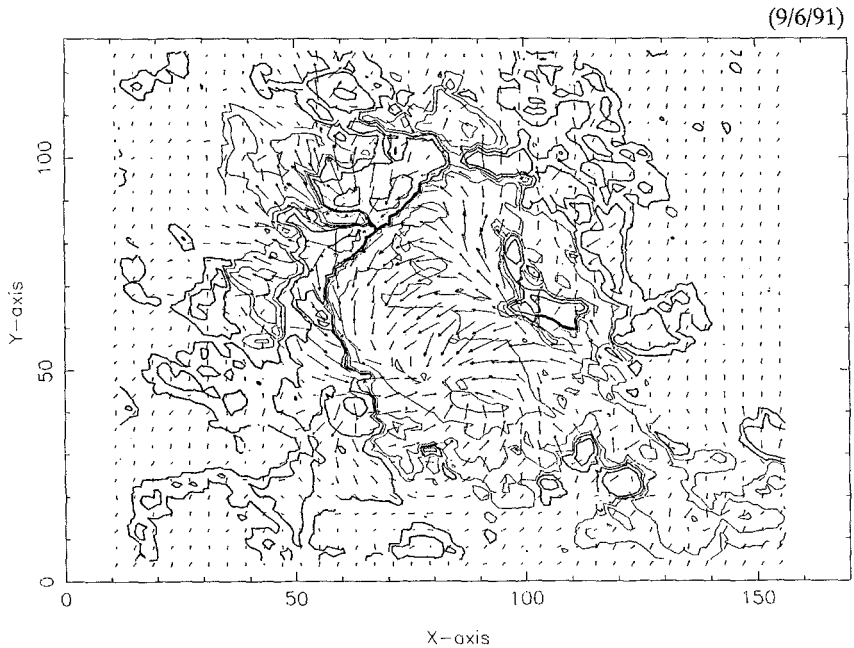

Fig. 2c.

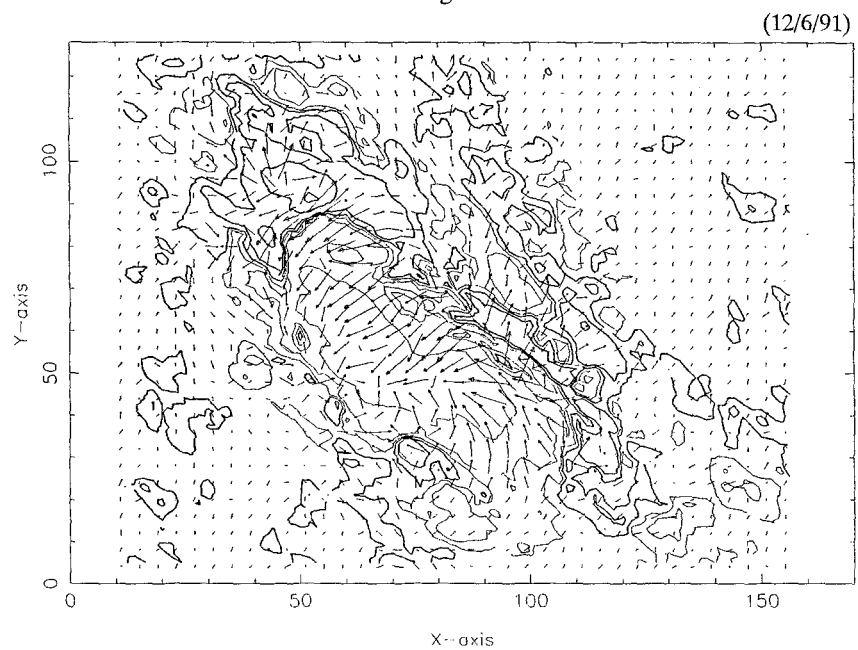

Fig. 2d.

Fig. 2a–d. Observed photospheric vector magnetic field distributions on (a) June 6, (b) June 8, (c) June 9, and (d) June 12, 1991 of AR 6659 by Huairou Solar Observing Station with the tangential ambiguity resolved. The unit length is 1367 km, about 1.8 arc sec. The longitudinal component is represented by iso-magnetic field contours with thick (thin) lines indicating N (S) polarity of the values ±40, ±160, ±640, ±1280, ±1920, ±2240, ±2560, and ±2880 G, whereas the transverse components are represented by arrow bars, with each length indicating the transverse field value at a scale of 250 G per unit length.

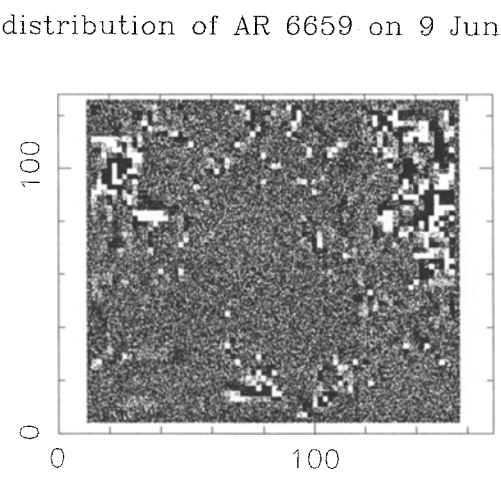

Fig. 3. Two-dimensional distribution of the force-free factor α of AR 6659 on 9 June, 1991 as a function of locations (x, y) in a grey map ranging from -10 A (black) per unit length (= 1367 km) to 10 A (white) per unit length.

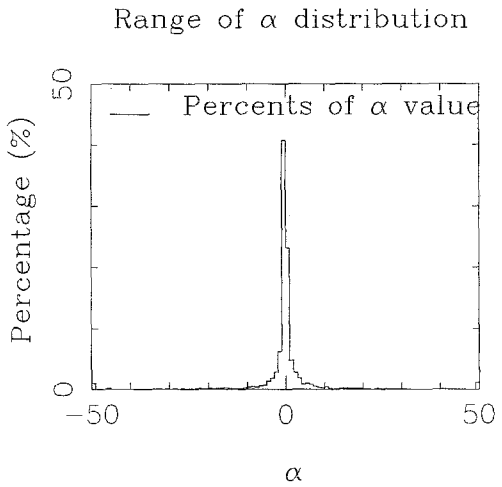

Fig. 4. Percentage distribution of α values in the magnetogram area of AR 6659 on 9 June, 1991. The unit of α is expressed as ampère per unit length (1367 km).

Since the location of the magnetogram area on 9 June, 1991 is closest to the disk center, or the central meridian, we have employed the magnetogram to evaluate the force-free factor, and this gives an average of $\alpha \approx 0.05$ A per unit length, or $\alpha \approx 3.6 \times 10^{-5}$ A km^{-1}. Figure 3 shows the grey-scale map of α distribution, and Figure 4 shows the percentage distribution of the α values. It can be seen that in most parts of the region α varies rather smoothly, though it is a function of location.

We proceed to extrapolate the magnetic fields in the solar atmosphere from the above vector magnetograms. Next we introduce the method employed.

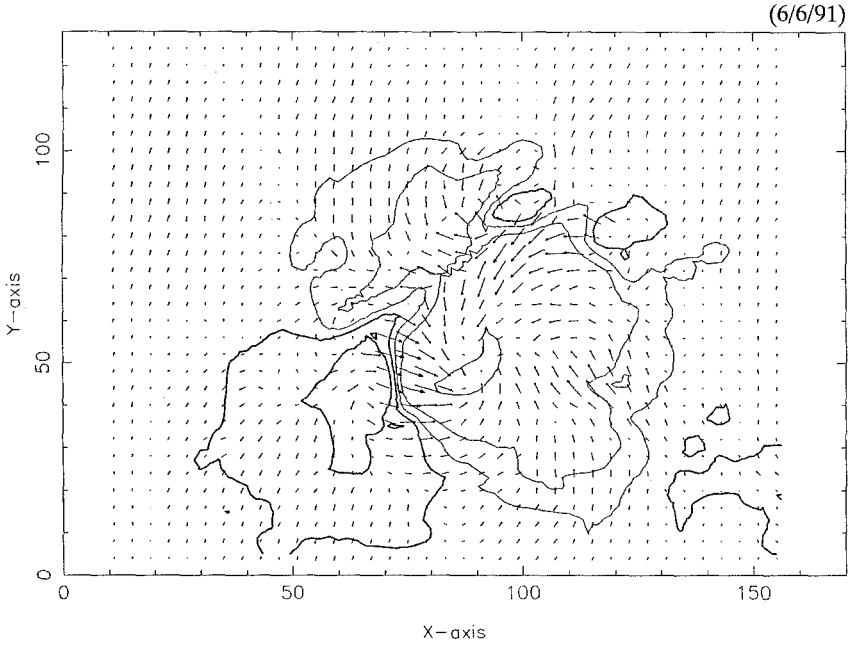

Fig. 5a.

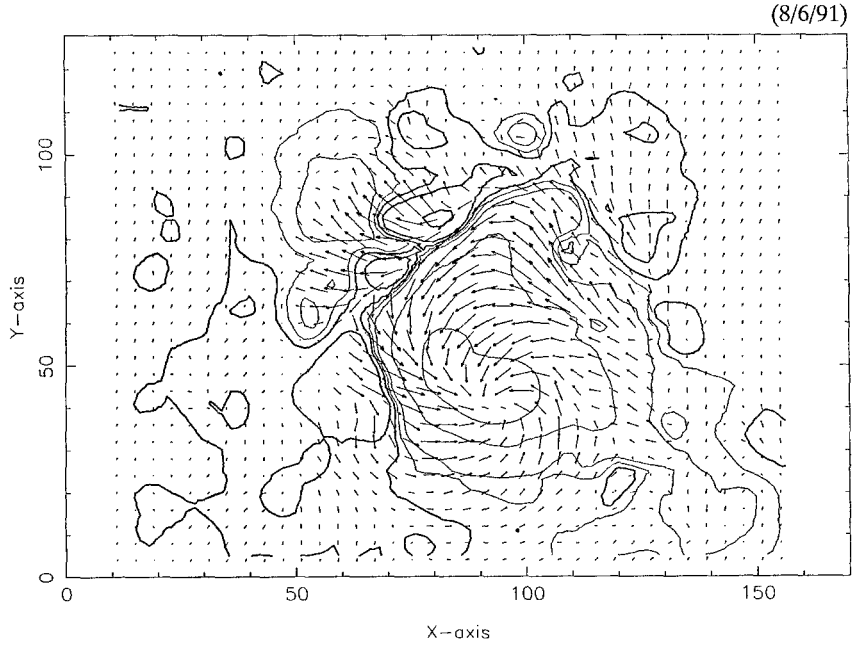

Fig. 5b.

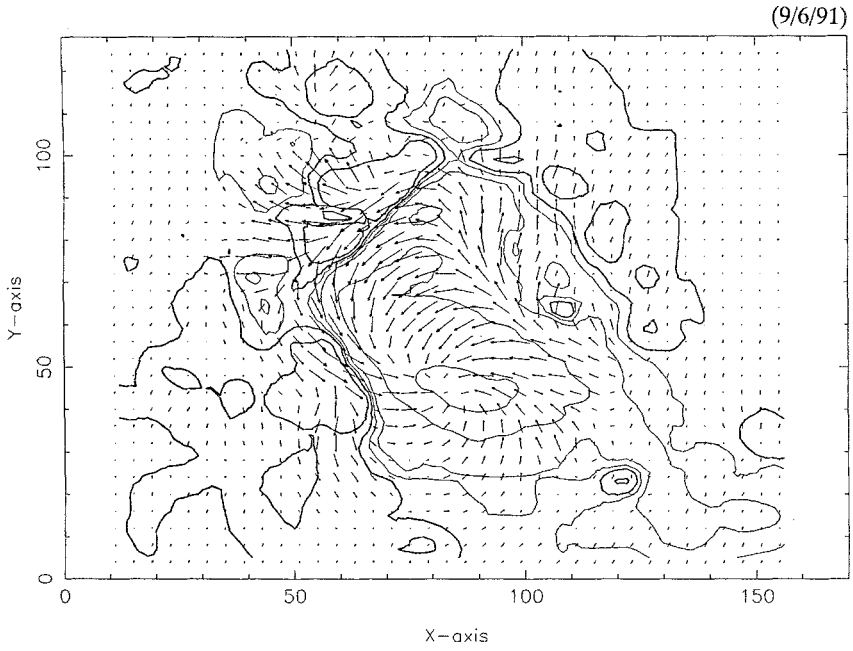

Fig. 5c.

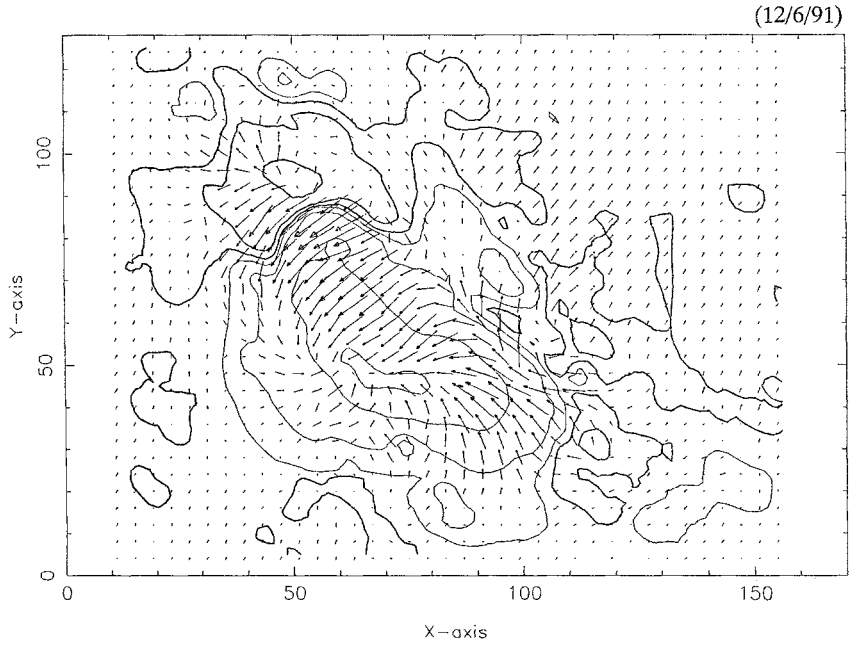

Fig. 5d.

Fig. 5a–d. Calculated vector magnetic field distributions in the chromosphere (the height is 2500 km measured from the bottom of the photosphere) on (a) June 6, (b) June 8, (c) June 9, and (d) June 12, 1991 of AR 6659, corresponding to the boundary conditions given in Figure 2(a–d), respectively. The longitudinal and transverse components are represented in the same way as in Figure 1.

3. Proposed Model and Implementation

We will use the formulation previously proposed by Yan, Yu, and Kang (1991), and improved in Yan (1995), where its properties and implementation were discussed in detail, to extrapolate magnetic fields above the solar surface. For the sake of consistency, the formulation is briefly described as follows.

Above and on the solar surface, $\mathbf{B}$ yields the following equations:

$$\left.\begin{array}{lll} \nabla \cdot \mathbf{B} = 0\,, \quad \nabla \times \mathbf{B} = \alpha \mathbf{B} & \text{in} & \Omega\,, \\ \mathbf{B} = \mathbf{B}_0 & \text{on} & \Gamma\,, \\ \mathbf{B} = O\left(\frac{1}{r^2}\right) & \text{when} & r \to \infty \end{array}\right\} \tag{1}$$

for a force-free magnetic field, where α is a constant, Ω is the space above the Sun, and Γ is the photosphere surface. $\mathbf{B}_0$ denotes known boundary values which are obtained consistently from observed vector magnetograms (Yan, 1995).

Then the above boundary value problem (1) has an unique finite energy solution, and its boundary integral representation is expressed as follows (Yan, 1995):

$$c_i \mathbf{B}_i = \int_\Gamma \left(F \frac{\partial \mathbf{B}}{\partial n} - \mathbf{B} \frac{\partial F}{\partial n} \right) \mathrm{d}\Gamma\,, \tag{2}$$

where c_i is a constant depending upon the location of the point i and F is the fundamental solution of the Helmholtz equation (Stratton, 1941). The integration is in the sense of a Cauchy principal value (Brebbia, Telles, and Wrobel, 1984).

The above integral equation can be solved numerically using BEM. In our case the element is simply formed from the magnetogram mesh, thus the computing resolution is comparable to the observational one. Then bi-quadratic shape functions are used to represent both the geometry and functions on each element. Introducing these representations into Equation (2), and transforming from the surface to intrinsic coordinates (ξ, η) defined for each element, we obtain the following discrete version of the equation, one for each boundary node:

$$\begin{aligned} c_i \mathbf{B}_i + \sum_{e=1}^{M} \sum_{k=1}^{9} \left[\int_{-1}^{+1} \int_{-1}^{+1} \frac{\partial F}{\partial n} N_k(\xi, \eta) J(\xi, \eta)\, \mathrm{d}\xi\, \mathrm{d}\eta \right] \mathbf{B}_k^e = \\ = \sum_{e=1}^{M} \sum_{k=1}^{9} \left[\int_{-1}^{+1} \int_{-1}^{+1} F N_k(\xi, \eta) J(\xi, \eta)\, \mathrm{d}\xi\, \mathrm{d}\eta \right] \left(\frac{\partial \mathbf{B}}{\partial n} \right)_k^e\,, \end{aligned} \tag{3}$$

where M is the number of total boundary elements, $\mathbf{B}_k^e$ and $(\partial \mathbf{B}/\partial n)_k^e$ are nodal values of $\mathbf{B}$ and $\partial \mathbf{B}/\partial n$ respectively, superscript e denotes the element, $N_k(\xi, \eta)$ are the bi-quadratic functions, and $J(\xi, \eta)$ denotes the Jacobian (Yan, 1995).

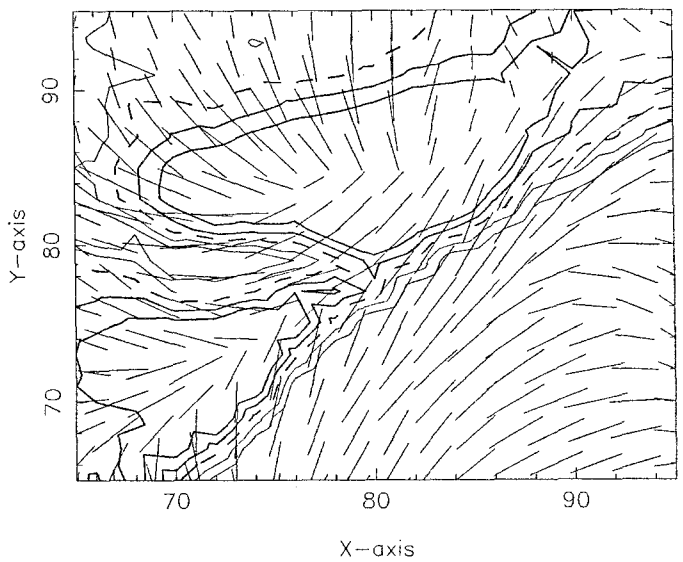

Fig. 6a.

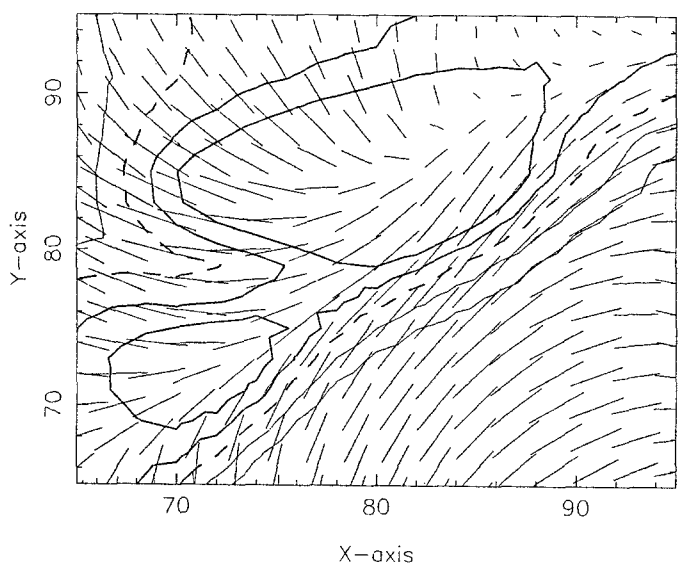

Fig. 6b.

Fig. 6a–b. Local vector magnetic fields (arrows have been omitted) in a flare-productive area in (a) the photosphere and (b) the chromosphere on June 8, 1991. The longitudinal component is represented by iso-magnetic field contours with thick (thin) solid lines indicating N (S) polarity of the values ± 160 G and ± 320 G, and dashed lines indicating the neutral line. The transverse components are represented by arrow bars with each length indicating the transverse field value at a scale of 500 G per unit length.

Fig. 7a.

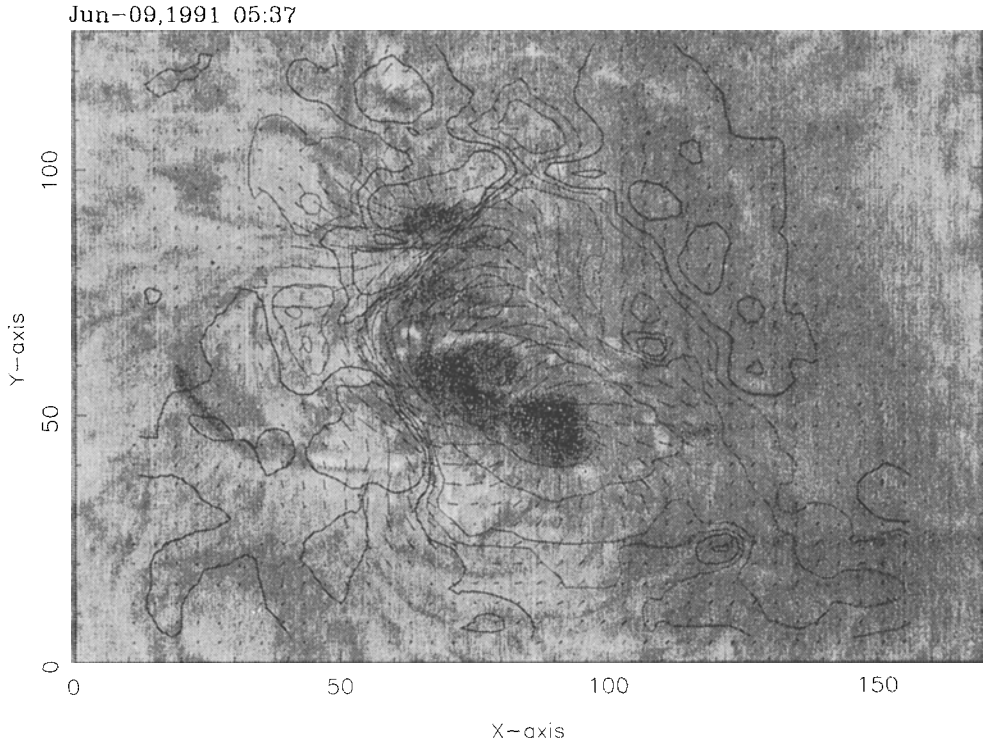

Fig. 7b.

Fig. 7a–b. (a) Observed chromospheric monochromatic Hβ image taken at 4861 Å of AR 6659 on June 9, 1991 by Huairou Solar Observing Station (courtesy H. Zhang). (b) The Hβ image is overlaid with the calculated vector magnetic fields.

This equation can be written in a matrix form, with the result of each integration forming a coefficient of [**H**] and [**G**] matrices (Brebbia, Telles, and Wrobel, 1984),

$$[\mathbf{H}]\{\hat{\mathbf{B}}\} = [\mathbf{G}]\left\{\frac{\widehat{\partial \mathbf{B}}}{\partial \mathbf{n}}\right\}, \tag{4}$$

where $\{\hat{\mathbf{B}}\}$ and $\{\widehat{\partial \mathbf{B}}/\partial n\}$ are vectors of nodal values. At each node $\mathbf{B}$ is known (as given by the boundary condition). Solution of the above equation permits unknown values to be determined consistently (Yan, Yu, and Yang, 1991).

It should be noted that in the BEM analysis, for a flat boundary, diagonal coefficients, which are singular integrals of the matrix [**H**], are zero prior to the value c_i of the free term of Equation (2). Diagonal coefficients of the matrix [**G**], however, have to be evaluated by the Gaussian integration scheme as discussed above. If a field point is lying on a plane element the corresponding coefficients of [**H**] also vanish to zero, otherwise the Gaussian integration scheme has to be performed (Yan, 1995).

4. Results and Discussions

Each magnetogram in the front view of Figure 1 comprises an area of $\Gamma_m = \{(x, y)|, 1 \leq x \leq 170, 1 \leq y < 128\}$. The unit length adopted there is 1367 km, and a mesh with 25×21 nodes and 120 nine-point bi-quadratic elements is employed, which covers one nineth of the computing area: $\Gamma = \{(x, y)|, 11 \leq x \leq 155, 4 \leq y \leq 124\}$, extracting from the magnetogram area, Γ_m. Thus the computation resolution is about 2733 km.

Figure 5(a–d) shows the calculated vector magnetic field distributions in chromosphere on 6, 8, 9, and 12 June, 1991, respectively, corresponding to the boundary conditions given in Figure 2(a–d), respectively, The longitudinal and transverse components are represented in the same way as in Figure 1. The height is 2500 km measured from the bottom of the photosphere.

Figure 6 demonstrates magnified vector magnetic fields (arrows have been omitted) in the local area extracted from Figures 2(b) and 5(b), where flares occurred. Figure 7 shows the observed chromospheric monochromatic Hβ image on 9 June, 1991 by Huairou Solar Observing Station, and the comparison with the calculated vector magnetogram in the chromosphere.

From the above comparison we can get the following features:

(1) The calculated transverse magnetic fields skew highly from the photosphere to the chromosphere at the following positive polarity spot (Figure 6) whereas they skew only slightly at the main preceding spot (Figure 5). This suggests that more energy was stored in the former area.

(2) At the umbra of the main preceding spot, anti-clockwise rotating magnetic fields are obtained, indicating that the outward electric currents flow from the solar surface to the solar atmosphere at the spot center.

(3) At the spot boundary, the plages agree well with the longitudinal magnetic field.

(4) The penumbral fibrils agree well with the transverse magnetic fields.

(5) The network structure is properly represented by the longitudinal component distribution.

(6) The filament is dominated by the transverse component.

Those results demonstrate the validity of our BEM solution and the associations between the force-free magnetic field and the structure of the AR 6659 region. In summary, while the AR 6659 is a very dynamic, flare-productive region, the constant-α, force-free magnetic field approximation can give fairly satisfactory results. Thus it is possible for us to evaluate the free energy stored between a non-constant-α magnetic field and a constant-α magnetic field.

Acknowledgements

This work was supported by China NNSF grant 49391400.11 and Chinese Academy of Sciences in part. We thank the Huairou Solar Observing Station for providing magnetogram data, Prof. H. Zhang for providing the Hβ filtergram, and Prof. J. Wang for helpful discussions.

References

Brebbia, C. A., Telles, J. C. F., and Wrobel, L. C.: 1984, *Boundary Element Techniques*, Springer-Verlag, Berlin.

Priest. E. R.: 1982, *Solar Magnetohydrodynamics*, D. Reidel Publ. Co., Dordrecht, Holland.

Stratton, J. A.: 1941, *Electromagnetic Theory*, McGraw-Hill, New York.

Wang, H.: 1993, in H. Zirin, G. Ai, and H. Wang (eds.), 'The Magnetic and Velocity Fields of Solar Active Regions', *IAU Colloq.* **141**, 323.

Yan, Y.: 1995, *Solar Phys.* **159**, 97. (This issue.)

Yan, Y., Yu, Q., and Kang, F.: 1991, *Solar Phys.* **136**, 195.

Zhang, H. and Wang, T.: 1994, *Solar Phys.* **151**, 129.

Zirin, H. and Wang, H.: 1993, *Nature* **363**, 426.